Water Research 115 (2017) 111–119

Contents lists available at ScienceDirect

Water Research

journal homepage: www.elsevier.com/locate/watres

Electrolysis-assisted mitigation of reverse solute flux in a three-chamber forward osmosis system

Shiqiang Zou, Zhen He*

Department of Civil and Environmental Engineering, Virginia Polytechnic Institute and State University, Blacksburg, VA 24061, USA

ARTICLE INFO

Article history:
Received 8 December 2016
Received in revised form
21 February 2017
Accepted 25 February 2017
Available online 28 February 2017

Keywords:
Forward osmosis
Electrolysis
Reverse solute flux
In-situ mitigation
Energy consumption

ABSTRACT

Forward osmosis (FO) has been widely studied for desalination or water recovery from wastewater, and one of its key challenges for practical applications is reverse solute flux (RSF). RSF can cause loss of draw solutes, salinity build-up and undesired contamination at the feed side. In this study, *in-situ* electrolysis was employed to mitigate RSF in a three-chamber FO system ("e-FO") with Na_2SO_4 as a draw solute and deionized (DI) water as a feed. Operation parameters including applied voltage, membrane orientation and initial draw concentrations were systematically investigated to optimize the e-FO performance and reduce RSF. Applying a voltage of 1.5 V achieved a RSF of 6.78 ± 0.55 mmol m^{-2} h^{-1} and a specific RSF of 0.138 ± 0.011 g L^{-1} in the FO mode and with 1 M Na_2SO_4 as the draw, rendering ~57% reduction of solute leakage compared to the control without the applied voltage. The reduced RSF should be attributed to constrained ion migration induced by the coactions of electric dragging force (≥1.5 V) and high solute rejection of the FO membrane. Reducing the intensity of the solution recirculation from 60 to 10 mL min^{-1} significantly reduced specific energy consumption of the e-FO system from 0.693 ± 0.127 to 0.022 ± 0.004 kWh m^{-3} extracted water or from 1.103 ± 0.059 to 0.044 ± 0.002 kWh kg^{-1} reduced reversed solute. These results have demonstrated that the electrolysis-assisted RSF mitigation could be an energy-efficient method for controlling RSF towards sustainable FO applications.

1. Introduction

Osmotically driven membrane processes are being developed to address global freshwater shortage, wastewater reuse and water-energy nexus (Cath et al., 2013; Ng et al., 2006). Among those processes, forward osmosis (FO) uses osmotic pressure gradient across a semi-permeable membrane to reclaim high-quality water for versatile applications, such as irrigation, food processing and life support (Cath et al., 2006). The major advantages of FO-based water treatment systems include reduced operating pressure, high rejection of undesired compounds, low fouling intensity of FO membranes, and less energy demand if energy-intensive draw regeneration can be properly addressed (Liu et al., 2011; Su et al., 2012).

A key challenge and also impediment for FO applications is the reverse solute flux (RSF) (Achilli et al., 2009; Hancock and Cath, 2009). RSF is defined as the cross-membrane diffusion of draw solutes to the diluted feed, and can result in severe loss of draw solutes and gradual salinity build-up at the feed side, leading to reduced osmotic driving force, increased fouling propensity, and elevated operation cost due to periodical replenishment of draw solutes (Achilli et al., 2010; Boo et al., 2012). Accumulation of the reversed draw solutes will require further treatment of the feed solution before it can be discharged to a natural water body (Phillip et al., 2010). Thus, mitigation of solute accumulation at the feed side is important, and several approaches have been proposed and studied, including the use of microorganisms to biologically degrade specific draw solutes in the feed, such as NH_4^+, NO_3^-, VFAs and EDTA, (e.g. anammox and osmotic membrane bioreactor, OMBR) (Holloway et al., 2015; Li et al., 2015), and continuous desalination of the concentrated feed through integrated electro-dialysis (ED), filtration (e.g., microfiltration), and/or bio-electrochemical systems (BES) with recoverable draw solutes (Lu and He, 2015; Luo et al., 2015; Qin and He, 2014). Although those methods can effectively reduce salinity accumulation at the feed side, they cannot mitigate or reduce RSF. Alternatively, novel membrane fabrication/modification methods can render reduced RSF, such as chemically cross-linked layer-by-layer polyelectrolytes and biomimetic membrane embedded with Aquaporin Z (Qiu et al.,

* Corresponding author.
E-mail address: zhenhe@vt.edu (Z. He).

http://dx.doi.org/10.1016/j.watres.2017.02.060
0043-1354/

2011; Wang et al., 2012). However, a notable trade-off between RSF and water flux as well as unsatisfied mechanical strength were observed in these modified membranes (Chung et al., 2012a).

The researchers have also attempted to decrease RSF through selection of appropriate draw solutes. Inorganic solutes were extensively investigated in FO systems, and the candidates with a lower ratio of RSF to water flux (J_s/J_w) were of great interest (Table S1, Appendix. A Supplementary Materials) (Achilli et al., 2010). It was reported that multivalent ions with larger hydrated radii, e.g. PO_4^{3-}, Ca^{2+}, and Mg^{2+}, could exhibit a lower cross-membrane diffusion rate and hence decrease solute leakage (Achilli et al., 2010; Nguyen et al., 2015). However, they could serve as the precursor of inorganic scaling, leading to severe membrane fouling (Phillip et al., 2010). The viability of some low J_s/J_w solutes, for instance $MgSO_4$, was hindered by their relatively high specific cost ($7.35 to make 1-L draw solution with an osmotic pressure of 2.8 MPa) (Achilli et al., 2010). Magnetic nanoparticles were also proposed as an emerging solute because they exhibited low RSF and could be separated by magnetic field and/or ultrafiltration (Ling and Chung, 2011a, b). Nonetheless, agglomerated nanoparticles required further ultrasonication for performance recovery, leading to weakened magnetic properties (Chung et al., 2012b; Ling et al., 2010).

Given the importance of RSF to FO applications, there is a critical need for developing effective methods to reduce RSF (Zou and He, 2016). In our previous study, a hybrid OMBR-ED system was developed for efficient draw solute recovery and mitigation of salinity build-up at the feed side (Lu and He, 2015). In an ED module, migration of ions across the ion-exchange membranes is achieved under the applied electric field. Herein, we employed the concept of electrolysis to an FO system for *in-situ* reduction of RSF. This electrolysis-assisted FO (e-FO) system contained two draw chambers (hydraulically connected) and one feed chamber; such a design was to minimize the effect of pH on the electrodes. Na_2SO_4 was chosen as a draw solute due to its relatively low specific cost, desired J_s/J_w ratio (half of the commonly adopted NaCl under same osmotic pressure, Table S1) and stable chemical property (cannot be electrolyzed in a solution). The specific objectives of this study were to (1) demonstrate the effectiveness of applied voltage on reducing RSF; (2) examine the ion migration pattern and other key performance parameters, such as water flux, recirculation rate, and fouling intensity; and (3) analyze energy consumption by electrolysis and system operation. To the best of our knowledge, this is the first study accomplishing *in-situ* RSF reduction in FO systems through operational strategies.

2. Materials and methods

2.1. e-FO system setup and operation

The three-chamber e-FO system consisted of two bilateral draw chambers (hydraulically connected) and one middle feed chamber (Fig. 1). Two pieces of cellulose triacetate (CTA) membranes with a total surface area (S) of 0.0032 m^2 (Hydration Technologies Inc., Albany, OR, USA) were installed with their active layers facing the feed (FO mode), creating an identical volume of 16 mL for each chamber (4 × 4 × 1 cm). Two stainless steel meshes (4 × 4 cm, ~1.4 cm distance), acting as both the electrode and swelling control, were placed close to the FO membrane (~0.2 cm) in the draw chambers and connected to an external power supply (CSI3644A, Circuit Specialists, Inc., Mesa, AZ, USA).

During operation, 200 mL of 1-M Na_2SO_4 (conductivity 87.1–88.4 mS cm^{-1}) was used as a draw solution; the effluents from both draw chambers were mixed and then recirculated back to the draw chambers. Deionized (DI) water was used as the feed solution and recirculated between the feed chamber and an external storage bottle; DI water was supplemented periodically to maintain a constant liquid volume of 500 mL. For each batch test, the e-FO system was operated for 24 h with water sampled every hour for the first 6-h operation and at the end of each test. The experiment was operated without any biological activities and in a temperature-controlled lab (20 ± 2 °C).

2.2. Experimental procedure

The feasibility of the e-FO system was first examined with an external voltage supply of 0 V (control system) and 3 V (experiment system), respectively. No voltage was applied to both systems in the first hour. When some solute ions gradually migrated to the feed side due to RSF, the feed conductivity was expected to increase and then the external power supply was turned on (at the end of the first hour) for the experiment system. The recirculation rate was set at 60 mL min^{-1} (4 cm s^{-1}) for all the draw and feed chambers in the feasibility test (Table S2). A series of system optimizations were then performed for the e-FO in terms of applied voltage (1 V, 1.5 V, 2 V and 3 V), membrane orientation (active layer facing feed and draw, i.e. FO and PRO mode), and initial draw concentration (0.5 M, 1 M, and 1.5 M) (Table S2). Fouling situation of the FO membrane was studied through monitoring water flux performance in three successive batch tests (24 h, FO mode) with 1 M Na_2SO_4 (200 mL) as the draw and DI water as the feed (500 mL constant). Because Na_2SO_4 was the only solute involved, fouling was mainly expected on the porous supportive layer (draw chamber, FO mode). Effective removal of residual foulants was achieved by i*n-situ* osmotic backwashing: DI water (1 L) and 1 M Na_2SO_4 (200 mL) were pumped into the draw and the feed chambers, respectively, for 6 h, followed by 30 min rinse with DI water.

2.3. Measurement and analysis

The detailed methods for water quality analysis were provided in the Supplementary Materials. The voltage across the external resistance (1 Ω) in the circuit was recorded every 2 min by a digital multimeter (Keithley Instruments Inc., Cleveland, OH, USA). Water flux was determined by measuring the change of water weight on an electronic balance (Scort Pro, Ohous, Columbia, MD, USA) at a 30-s interval according to a previous study (Yuan et al., 2016). Quantification of water flux was based on Eqs. S1–S3 (Supplementary Materials). Flux recovery rate in fouling test was calculated as the ratio of maximum water flux (in the first hour) between backwash and pristine membranes. The solute build-up (SBU) at the feed side was quantified by Eq. (1) with a unit of mmol m^{-2} h^{-1} (Zou and He, 2016). SBU is typically resulted from the concentrating effect in the feed (due to membrane rejection of the feed solute) and reverse solute flux (RSF, mmol m^{-2} h^{-1}) from the draw solution (Phillip et al., 2010). When DI water is used as the feed, $C_{i,F} = 0$ and hence no concentrating effect is observed. Under such a case:

$$SBU = RSF = \frac{n_{f,F} - n_{i,F}}{S \times t} = \frac{V_F \times \left(C_{f,F} - C_{i,F}\right)}{S \times t} \quad (1)$$

where $n_{i,F}$ and $n_{f,F}$ are initial and final mole of Na_2SO_4 in the feed, respectively. $C_{i,F}$ and $C_{f,F}$ are initial and final Na_2SO_4 concentration in the feed, respectively. V_F is feed volume (500 mL constant). t (h) stands for operating time. S (m^2) is the total surface area of the FO membrane. Specific RSF (g L^{-1}) was also calculated for comparison with previous studies (Phillip et al., 2010), and defined as the ratio of J_s (g $m^{-2}h^{-1}$, GMH) and J_a (LMH):

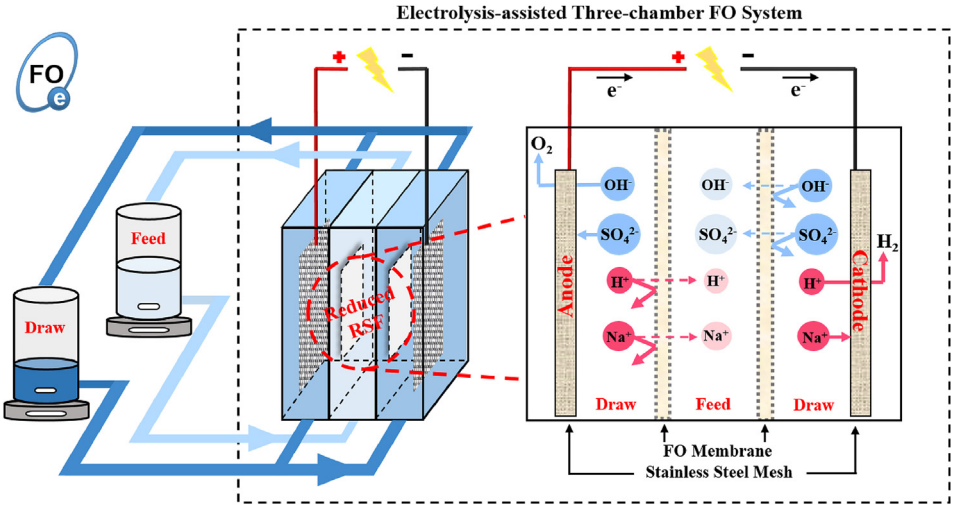

Fig. 1. Schematic of the electrolysis-assisted three-chamber forward osmosis system.

$$Specific\ RSF = \frac{J_s}{J_a} = \frac{RSF \times Mw}{J_a \times 1000} \quad (2)$$

Based on water flux performance together with the reduced reverse solute, energy consumption of the e-FO system was evaluated either with different voltage (1 V, 1.5 V, 2 V and 3 V) or different recirculation rate (10 mL min^{-1}, 30 mL min^{-1} and 60 mL min^{-1} for all chambers). The energy consumption rate was normalized either by unit recovered water or unit reduced reverse solute. It is assumed that the power consumption of the e-FO system is mainly attributed to the recirculation pump and the power supply. The specific energy consumption (SEC) for unit recovered water (E_w, kWh m^{-3}) is estimated as (Shaffer et al., 2012):

$$E_w = \frac{P_{system}}{Q} \approx \frac{P_{pump} \times \rho}{m_{t,D} - m_{t-1,D}} or \frac{\left(P_{pump} + P_{electricity}\right) \times \rho}{m_{t,D} - m_{t-1,D}} \quad (3)$$

where P_{pump} (kW) and $P_{electricity}$ (kW) are the power consumption of the recirculation pump and external voltage supply, and Q (m^3 h^{-1}) is recovered water flow rate. $m_{t,D}$ and $m_{t-1,D}$ represent the mass of draw solution at a specific time t and t-1 (h), respectively.

The SEC for unit reduced solute (E_s, kWh kg^{-1}) is defined as the amount of reduced reverse solute because of external power supply and estimated as:

$$E_s = \frac{P_{electricity} \times t}{\Delta m_{solute,f}} = \frac{P_{electricity} \times t}{m_{solute,control.f} - m_{solute,experiment.f}} \quad (4)$$

where $\Delta m_{solute,\ f}$ (kg) is the reduced solute mass due to applied voltage by comparing the control ($m_{solute,control.f}$) and the experiment groups ($m_{solute,experiment.f}$). The SEC for unit reduced solute based on the entire e-FO system ($E_{s,total}$, kWh kg^{-1}) is determined by:

$$E_{s,total} = \frac{\left(P_{pump} + P_{electricity}\right) \times t}{m_{solute,control.f} - m_{solute,experiment.\ f}} \quad (5)$$

3. Results and discussion

3.1. Feasibility of the e-FO system

The feasibility of the e-FO system was investigated for its water flux performance, RSF reduction, and comparison with a two-chamber FO system that was also assisted by electrolysis. With an applied voltage of 3 V, the e-FO system generated comparable average water flux (maximum ~9.0 LMH) and the volume of the recovered water (~450 mL) within 24 h when compared to that with 0 V. However, a notable decrease in the conductivity of the final feed solution from 536 ± 12 (0 V) to 343 ± 9 μS cm^{-1} (3 V) was observed, rendering reduction of 35.9 ± 0.3%. The reduced conductivity should be primarily attributed to less reverse-fluxed solute from the draw, resulting in a mitigated RSF of 9.53 ± 0.49 mmol m^{-2} h^{-1} with 3 V, significantly lower than 15.57 ± 0.23 mmol m^{-2} h^{-1} with 0 V. Meanwhile, a more desired specific RSF (i.e. J_s/J_a) of 0.194 ± 0.010 g L^{-1} was achieved against the control system and that reported in the literature (0.320–0.330 g L^{-1}, Table S3). For comparison, a two-chamber conventional FO was examined with or without applied voltage (Fig. S1). The results show that the three-chamber e-FO system had merits in terms of water extraction capability, solution pH and system stability. The three-chamber e-FO system outcompeted the conventional two-chamber FO with a notable increase in the maximum water flux (tripled, Fig. S2A). When electrolysis (3 V) was applied to the two-chamber FO system, unbalanced pH in both the feed (3.02 ± 0.03) and the draw (10.70 ± 0.21) solutions was detected, which could cause the damage of electrodes and membrane in long-term operation; after 24-h operation, the elevated Fe^{3+} level (1.99 ± 0.53 mg L^{-1}) was detected in the final feed solution of the two-chamber FO system, indicating the corrosion of the anode electrode (Fig. S2C embedded). The three-chamber e-FO system, on the other hand, had very stable pH in both solutions (Fig. 2B). It was worth noting that the applied voltage induced an adverse effect in the two-chamber e-FO system with tripled feed conductivity (662 ± 4 μS cm^{-1} with 3 V vs. 227 ± 2 μS cm^{-1} with 0 V, Fig. S2C), indicating the increased ion concentration from elevated RSF and generated H^+/Fe^{3+} (Figs. S2B and S2C embedded). Hence, the three-chamber e-FO system offered cost-savings in long-term operation with advantages of higher water flux, less solute loss via reduced RSF, prolonged electrode lifespan and stable water quality (e.g. solution pH).

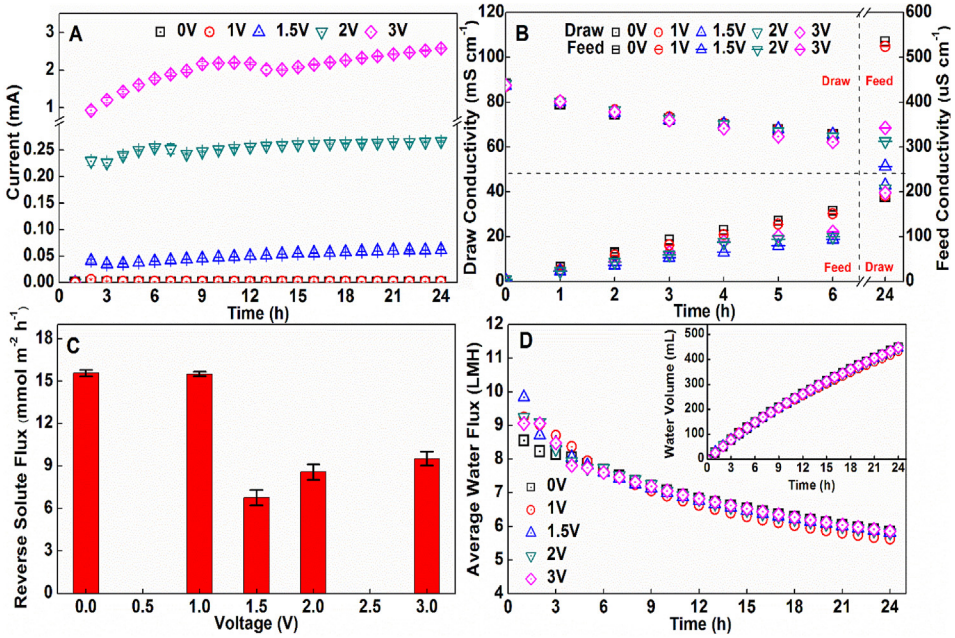

Fig. 2. The performance of the e-FO system under different applied voltages: (A) current generation; (B) conductivity variations in the draw and the feed solution; (C) reverse solute flux; and (D) water flux and the volume of the extracted water.

3.2. Effect of applied voltage

To better understand the effects of the applied voltage on electrolysis-assisted RSF mitigation, the external voltage was then successively reduced from 3 V to 2 V, 1.5 V, and 1 V. As a result, the current decreased from 2.04 ± 0.41 mA (3 V) to 0.26 ± 0.01 mA (2 V), and then 0.037 ± 0.001 mA (1.5 V) (Fig. 2A). Interestingly, with the decrease of the applied voltage from 3 V to 1.5 V, the electrolysis-assisted mitigation of RSF was enhanced, and the lowest conductivity of 257 ± 6 μS cm^{-1} in the final feed solution and the lowest RSF of 6.78 ± 0.55 mmol m^{-2} h^{-1} were achieved with 1.5 V (Fig. 2B and C). The specific RSF with 1.5 V (0.138 ± 0.011 g L^{-1}) was more than 70% lower than that of the control system (0 V) and the conventional cross-flow FO systems (Table S3). It should be noted that the theoretical thermodynamic voltage of water decomposition is 1.23 V, and a threshold voltage of 1.5 V should be expected for successful albeit limited electrolysis (Bockris et al., 1985), considering the overpotential effects (Wang et al., 2014b). Below the threshold voltage, extremely low current of 0.002 ± 0.001 mA and negligible production of H_2 and O_2 with 1 V indicated a failure of water splitting, supported by the previous study that detectable electrolysis-induced gas production occurred with at least 1.5 V (Tuna et al., 2009). As a result, no inhibition of RSF was expected with 1 V, which led to similar feed conductivity (525 ± 7 μS cm^{-1}) and RSF (15.51 ± 0.15 mmol m^{-2} h^{-1}) to those in the control system (0 V). Elevated initial water flux was observed in the first hour with a peak value appeared under 1.5 V (9.84 ± 0.37 LMH) compared to that under 0 V (8.06 ± 0.25 LMH, Fig. 2D). The overall average water flux and recovered volume was independent of the applied voltage with negligible water loss from the splitting reaction (estimated water loss in Supplementary Materials). No obvious temperature variations were detected in all water samples.

The reduced RSF should be attributed to ion migration induced by the coactions of both the effective electric field (≥1.5 V with water electrolysis) and high solute rejection of FO membrane. The e-FO system exhibited a similar process to that of ED, with H^+ reduction to H_2 at the cathode and OH^- oxidation to O_2 at the anode; meanwhile, Na^+ and SO_4^{2-} migrated from the draw solution into the feed solution driven by concentration gradients. With an applied voltage ≥1.5 V, the potential difference between the electrodes could generate a dragging effect that is highly-effective in retaining opposite-charged ions (anions at the anode and cations at the cathode), whereas an applied voltage < 1.5 V failed to maintain an effective dragging force with the absence of water splitting. However, unlike ED that is equipped with ion exchange membrane, the e-FO system contained FO membrane only allowing the draw solute ions to diffuse through by indirect partitioning, which is partially governed by a cross-membrane concentration gradient (Phillip et al., 2010). Thus, the same-charged ions (cations at the anode and anions at the cathode) will be repelled by the electrode (i.e. repelling effect), but fail to efficiently diffuse through the FO membrane due to membrane rejection. As a result, the higher voltage applied above 1.5 V, the faster same-charged ions will be accumulated at the boundary layer, which could exceed the reduced concentration of opposite-charged ions via dragging effect, eventually creating a larger concentration gradient together with diffusion force. This explanation is in accordance with the increased RSF and the conductivity of the final feed solution from 1.5 V to 3 V (Fig. 2B and C). The strengthened diffusion load of ions induced by the repelling effect can also lead to detectable fouling situation. For example, ~14% reduction in both water volume and maximum flux was observed with 3 V after three-time batch tests (Fig. S3). This reversible fouling could be controlled by osmotic backwashing with a recover rate of 98% (Le-Clech et al., 2005).

Cross-membrane migration of ions (Na^+, H^+, SO_4^{2-}, and OH^-) also led to pH variation in both the draw and feed solutions, highly depending on the applied voltage (Fig. 3A). According to the prior studies (Achilli et al., 2010; Phuntsho et al., 2011), multivalent ions with larger hydrated radii (Nightingale, 1959), such as PO_4^{3-} and SO_4^{2-}, exhibited lower diffusion rates compared to monovalent ions (e.g. K^+ and Na^+). Assuming 2 mol of Na^+ diffuse to the middle feed chamber, 1 mol of SO_4^{2-} should migrate at the same time; SO_4^{2-} may be partially substituted by OH^-, rendering a ratio of Na^+ to SO_4^{2-} larger than 2 (2.047 ± 0.003 with 0 V, Fig. 3B). Hence, this Na^+-

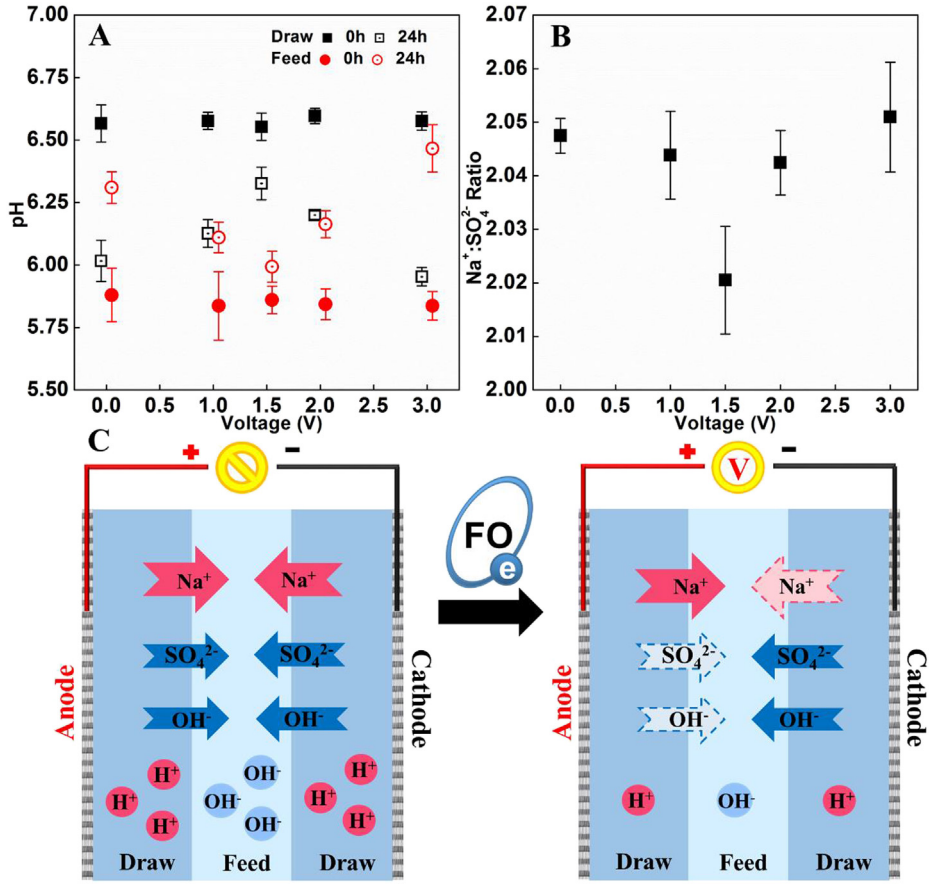

Fig. 3. The profiles of (A) pH variations; (B) ratio of Na^+ to SO_4^{2-}; and (C) proposed ion migration pattern.

governed diffusion, due to a higher cross-membrane concentration gradient of Na^+, will lead to excess diffusion of OH^- to the feed (0 V, Fig. 3C). This assumption was validated with pH increase in the feed (from 5.88 ± 0.11 to 6.31 ± 0.06) and corresponding pH drop in the draw solution (from 6.56 ± 0.07 to 6.02 ± 0.08), respectively (0 V, Fig. 3A). A comparable Na^+:SO_4^{2-} ratio of 2.044 ± 0.008 was observed with 1 V. However, when 1.5 V was applied to the e-FO system, the solution pH was affected to a less degree in both the feed (from 5.86 ± 0.06 to 5.99 ± 0.06) and the draw (from 6.55 ± 0.05 to 6.33 ± 0.07, Fig. 3A), and a Na^+:SO_4^{2-} ratio of 2.020 ± 0.010 was closer to the theoretical value (1.5 V, Fig. 3B), resulted from less migration of solute ions, especially Na^+ (Fig. 3C). With further increase of external voltage from 1.5 V to 3 V (accompanied by increasing current generation), the repelling effect might become dominant, leading to more Na^+ leakage (a Na^+:SO_4^{2-} ratio of 2.051 ± 0.010 at 3 V, Fig. 3B). This would enhance OH^- diffusion to neutralize the excess Na^+, rendering augmented pH variation with 3 V (Fig. 3A).

Although relatively stable solution pH was achieved by mixing the anolyte and the catholyte in the e-FO system, a high voltage (e.g., 3 V) could generate more H^+ inside the anode chamber, causing the undesired corrosion of the electrode (Fig. S4). Soluble iron (Fe^{3+}) was detected in the final draw solution with 3 V operation (1.50 ± 0.08 mg L^{-1}, Table S4), and this concentration could be higher with longer term of operation. Thus, a moderate voltage of 1.5 V, though relatively low in electrolytic efficiency of water splitting, would be more favored due to reduced solute leakage by dragging effect (56.5 ± 2.3% reduction for RSF and 56.8 ± 2.9% reduction for specific RSF compared to that with 0 V, Fig. 2C and Table S3), negligible water loss due to splitting reaction (<0.001 mL L^{-1} recovered water, Supplementary Materials), alleviated repellence of same-charged ions, and prolonging electrode lifespan. To avoid electrode corrosion during the long-term operation, the non-corrosive materials such as platinum and/or iridium may also be considered as the electrodes, though at a higher expense.

3.3. Effect of membrane orientation

The e-FO system was further investigated for the effect of the membrane orientation (FO vs. PRO mode) with an applied voltage of 0 V or 1.5 V. It was found that the PRO mode exhibited higher water flux (12.31 ± 0.25 to 12.97 ± 0.53 LMH), because of concentrative internal concentration polarization (ICP) and a larger effective osmotic gap ($\Delta\pi_{eff}$) (McCutcheon et al., 2006), than that of the FO mode (8.06 ± 0.29 to 9.84 ± 0.17 LMH, Fig. 4A). However, in the PRO mode, there was negligible difference in the conductivity of the final feed solution between 0 V (749 ± 8 μS cm^{-1}) and 1.5 V (755 ± 12 μS cm^{-1}, Fig. 4B), while significant reduction of RSF in the FO mode was observed with the draw conductivity decreasing from 536 ± 12 μS cm^{-1} with 0 V to 257 ± 6 μS cm^{-1} with 1.5 V. This could be explained by the voltage-affected ion diffusion pattern inside the asymmetric FO membrane (Fig. 4C). According to a previous study, diffusion of draw solute across the active layer (J_s^A) without an effective electric field (≥1.5 V in current case) can be calculated using Fick's law of diffusion (Eq. (6)) (Phillip et al., 2010).

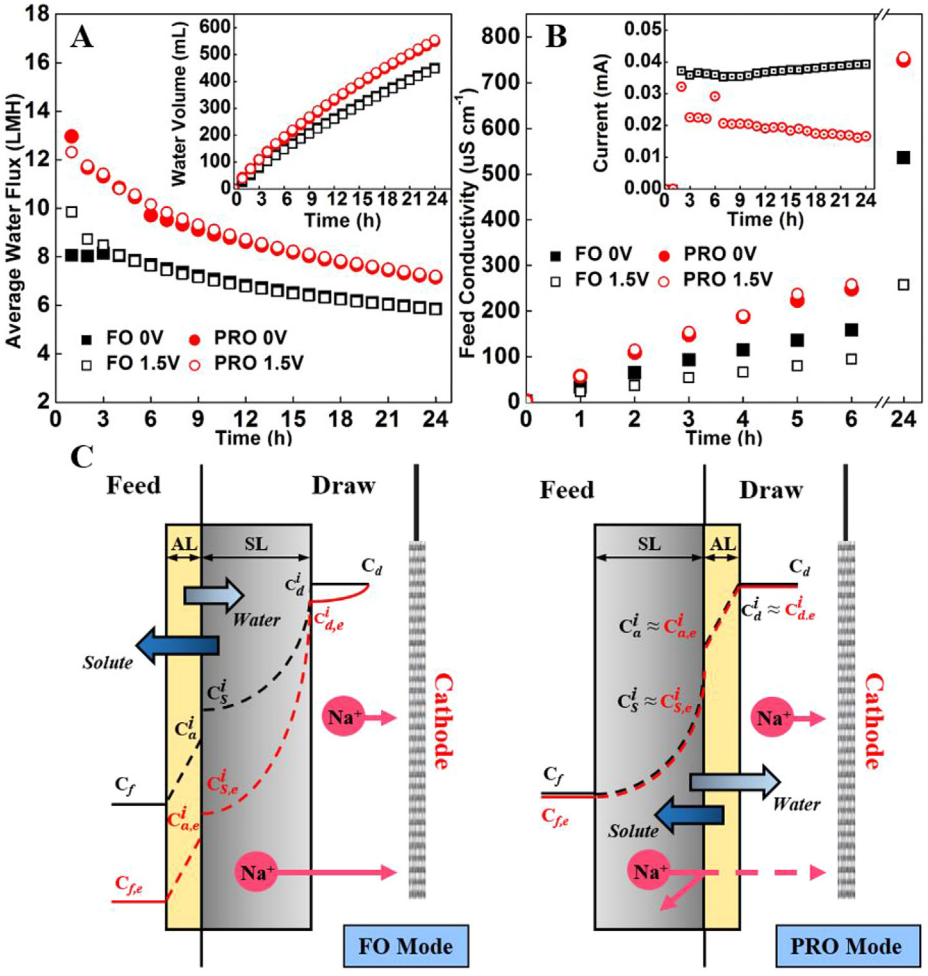

Fig. 4. The e-FO performance under two different membrane orientations, FO mode and PRO mode: (A) water flux; (B) conductivity and current variations in feed solutions; and (C) the proposed ion diffusion pattern inside asymmetric FO membrane. In Fig. 4C, the black line is the ion diffusion pattern without applied voltage (0 V), and the red line with a subscript "e" is the ion diffusion pattern with applied voltage (1.5 V). (For interpretation of the references to colour in this figure legend, the reader is referred to the web version of this article.)

$$J_s^A = -D^A\frac{dC}{dt} = -\frac{D^A}{t_A}\left(C_a^i - C_f\right) = -\frac{D^A}{t_A}\left(C_a^i - 0\right) \tag{6}$$

where D^A is the diffusion coefficient of draw solute in active layer, t_A is the thickness of active layer, C_a^i is the concentration of draw solute on the active layer side of the supportive layer-active layer interface, and C_f is the concentration of draw solute in the feed (assuming $C_f^i \approx C_f$ in an FO system with negligible external concentration polarization, ECP) (Cath et al., 2006). Initially, C_f equaled to 0 as DI was applied as the feed. Similarly, diffusion of draw solute across the supportive layer (J_s^S) can be quantified (Eq. (7), applied voltage <1.5 V).

$$J_s^S = -D^S\frac{dC}{dt} = -\frac{D^S}{t_S}\left(C_d^i - C_s^i\right) = -\frac{D^S}{t_S}\left(C_d - 0\right) \tag{7}$$

where D^S is the diffusion coefficient of draw solute in supportive layer, t_S is the thickness of supportive layer, C_s^i is the concentration of draw solute on the supportive layer side of the supportive layer-active layer interface (initially equals to 0), and C_d is the concentration of draw solute in the draw chamber (assuming $C_d^i \approx C_d$).

When an effective voltage (≥1.5 V) was exerted on the e-FO system, ion migration induced by the electric field should be taken into account together with ion diffusion in supportive layer. The modified ion transport ($J_{s,e}^S$) across the supportive layer can be calculated using Nernst-Plank equation (Eq. (8) with specified deduction in Supplementary Materials, initially $C_{s,e}^i = 0$).

$$J_{s,e}^S = -\frac{D^S}{t_S}\left(C_{d,e}^i - C_{s,e}^i - \frac{FzC_d}{RT}E\right) = -\frac{D^S}{t_S}\left(C_{d,e}^i - 0 - \frac{FzC_d}{RT}E\right) \tag{8}$$

Comparing Eqs. (7) and (8), when 1.5 V was exerted, Na^+ in both the draw solution and the supportive layer would migrate towards the cathode electrode, leading to a relatively lower concentration of the draw solute on the supportive layer ($C_{d,e}^i < C_d \approx C_d^i$) and hence reduced ion transport ($J_{s,e}^S < J_s^S$). Eventually, slower ion transport in active layer could be achieved under an effective electric field ($J_{a,e}^A < J_a^A$ under FO mode, detailed explanation in Supplementary Materials), resulting in reduced ion concentration in the feed chamber compared to that with 0 V over an extended period of time ($C_f^e < C_f$, FO mode, Fig. 4C).

When the active layer facing the draw (the PRO mode), only Na^+ in the bulk solution could be dragged towards the cathode electrode at the draw side, rendering a similar concentration on the interface ($C_d^i \approx C_{d,e}^i$ in the PRO mode; ECP was not considered, Fig. 4C). Hence, comparable solute concentrations on the

supportive side of supportive-active layer interface would be expected ($C^i_{s,e} \approx C^i_s$, the PRO mode, Fig. 4C). Despite the attempt of migration towards the cathode from the feed side, Na^+ in the supportive layer would be rejected by the active layer (the PRO mode, Fig. 4C), leading to similar ion diffusion in active layer ($J^A_{s,e} \approx J^A_s$). Failure of voltage-induced ion migration in PRO mode further rendered lower average current (0.020 ± 0.004 mA, 1.5 V, Fig. 4B embedded) compared to that in the FO mode (0.037 ± 0.001 mA, 1.5 V).

It should be noted that, although reduced RSF was achieved by the e-FO system in the FO mode, no significant difference in water flux and volume was observed after 24-h operation between 0 V and 1.5 V (Fig. 4A). According to Eqs. S1 and S2, water flux across the active layer can be quantified by Eq. (9).

$$Jw = A(\pi_D - \pi_F) = A\left(C^i_a - C_f\right)RT = A\left(C^i_a - 0\right)RT \quad (9)$$

In the FO mode, owing to the dragging effect, $C^i_{a,e}$ would be lower than C^i_a, leading to an immediate smaller $J_{w,e}$ than J_w. However, because of more draw solute diffusion to the feed with 0 V (larger loss), C^i_a would be expected to decrease relatively faster than $C^i_{a,e}$. These two contrary effects might have compensated each other during the long-term operation, resulting in comparable water flux and volume of the extracted water. Note that electro-osmosis was not considered in water flux because its major effect was to reduce concentration polarization (negligible in an FO process) by enhancing the fluid movement and thus mass transfer in the boundary layer (Liang et al., 2016).

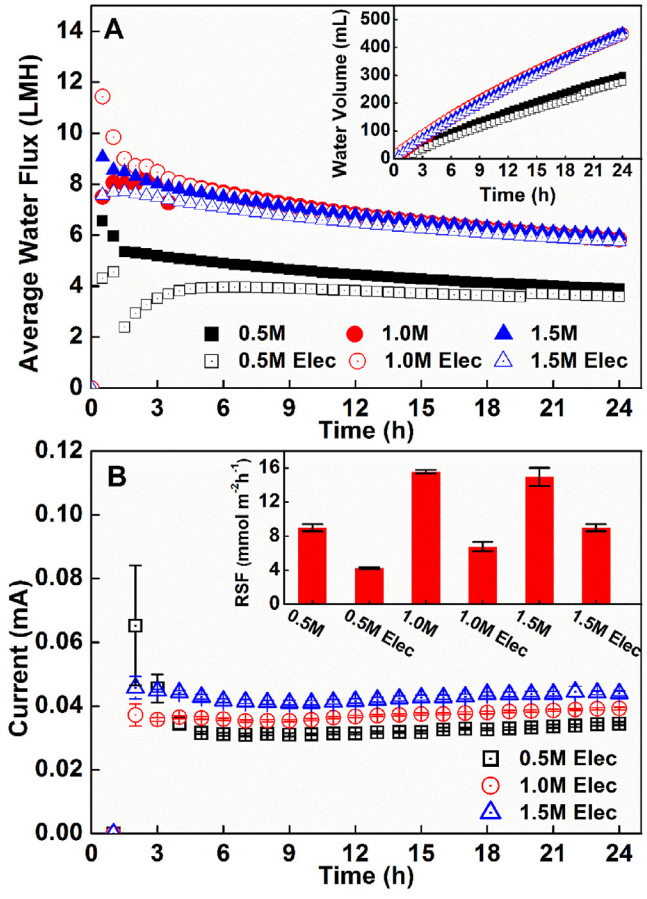

Fig. 5. Effects of the initial draw concentration with an applied voltage of 0 V or 1.5 V: (A) water flux and the volume of the collected water; and (B) current generation together with RSF under different initial draw concentration (inset).

3.4. Effect of initial draw concentration

In an FO system, both water flux and RSF are governed by the solute concentration gradient across FO membrane (Eqs. (6) and (9)). When the initial Na_2SO_4 concentration increased from 0.5 M to 1.0 M, water flux increased from 4.6 ± 0.6 LMH to 6.9 ± 0.7 LMH in 24 h, resulting in 150% increase in the volume of water extraction (Fig. 5A). However, further increasing the Na_2SO_4 concentration to 1.5 M did not increase water flux (6.9 ± 0.8 LMH). This may be attributed to non-linear correlation between osmotic pressure (i.e. driven force) and solute concentration at a higher concentration, suggesting a biased estimation of *van't Hoff equation* (Eq. S(2)) for "non-ideal" solutions (e.g. 1.5 M Na_2SO_4, almost saturated) (Cath et al., 2006). Efficient water permeation can also be hindered by ICP resulted from limited mass transfer in the supportive layer (Wang et al., 2014a). The comparable volume of water extraction led to similar conductivity of the final feed solution (after dilution with extracted water), 536 ± 12 μS cm^{-1} and 524 ± 33 μS cm^{-1}, by using 1.0 M and 1.5 M draw solutions, respectively (Phillip et al., 2010). The electrolysis-assisted mitigation of RSF was more pronounced at relatively lower initial draw concentrations (0.5 and 1.0 M). With an applied voltage of 1.5 V, the RSF was reduced by 52.8 ± 1.7% (0.5 M), 56.5 ± 2.3% (1.0 M), and 39.4 ± 6.9% (1.5 M), respectively, compared to that with 0 V (Fig. 5B embedded). This phenomenon could partially be attributed to a higher ion diffusion rate occurred at a larger concentration gradient. On the other hand, the dragging force provided by the electrode and electric field was rather similar among the three concentrations, indicated by comparable current generation over the 24-h operation: 0.034 ± 0.007 mA at 0.5 M, 0.037 ± 0.001 mA at 1.0 M, and 0.043 ± 0.001 mA at 1.5 M (Fig. 5B). Notable initial current fluctuation was observed with 0.5 M Na_2SO_4 as the draw, owning to a lower concentration and more significant concentration polarization near the electrode.

3.5. Energy consumption of the e-FO system

Although the FO process has been widely studied as an energy-efficient process, the information of energy consumption was rarely reported in the previous studies (Zou et al., 2016). In this e-FO system, energy was mainly consumed by the recirculation pumps and the external power supply. At a constant recirculation rate of 60 mL min^{-1}, the highest energy consumption was estimated to be 1.03 ± 0.26 kWh m^{-3} with the applied voltage of 3 V, among which 33.1% was attributed to power supply while the rest was used by the recirculation pump (inset, Fig. 6A). When the external voltage was reduced to 2 V, the energy consumption was decreased to 0.72 ± 0.13 kWh m^{-3}. Further reduction of the applied voltage to 1.5 and 1 V rendered a comparable energy consumption (0.69–0.72 kWh m^{-3}) to that with 0 V (0.69 ± 0.13 kWh m^{-3}), resulted from the dominant consumption by the recirculation pump (>96%) with 0–2 V (Fig. 6A inset). Thus, the effect of the recirculation rate was further investigated with an applied voltage of 1.5 V (Fig. 6B). Reducing the recirculation rate from 60 mL min^{-1} to 30 mL min^{-1} and finally 10 mL min^{-1} rendered similar FO performance (both water flux and final feed conductivity, Fig. S5), owning to negligible external concentration polarization (ECP) (Xie et al., 2015), but significantly reduced the energy consumption of the e-FO system. The highest recirculation rate of 60 mL min^{-1} resulted in an overall energy consumption of 0.69 ± 0.13 kWh m^{-3}, which was reduced to 0.18 ± 0.03 kWh m^{-3} at 30 mL min^{-1}. Further reduction of the recirculation rate to 10 mL min^{-1} exhibited the lowest energy consumption of 0.022 ± 0.004 kWh m^{-3} (13% by the

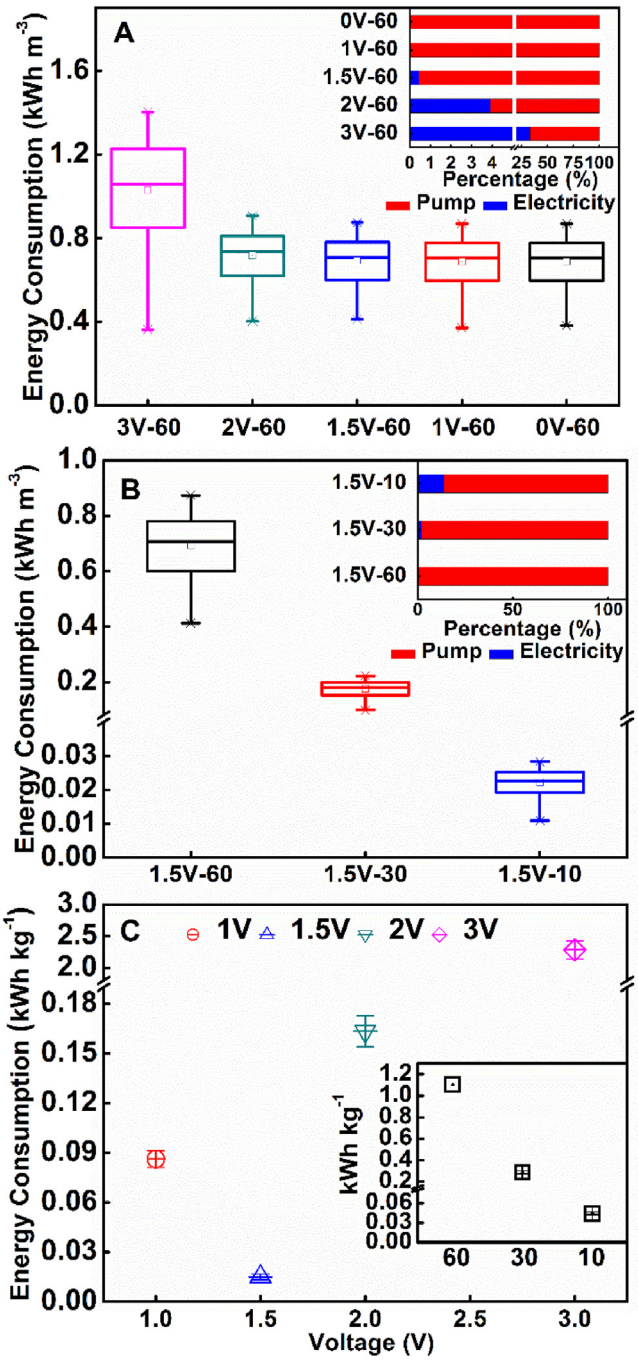

Fig. 6. Energy consumption by the e-FO system: (A) E_w under different applied voltages and a recirculation rate of 60 mL min^{-1}; (B) E_w under different recirculation rates and an applied voltage of 1.5 V; and (C) E_s under different voltage (main figure) and $E_{s,total}$ under different recirculation (60, 30 and 10 mL min^{-1}) with applied voltage of 1.5 V (inset). The "3V-60" stands for an applied voltage of 3 V and a recirculation rate of 60 mL min^{-1}.

power supply and 86% by the recirculation pump, Fig. 6B inset), which was about 3.2% of the energy consumption with 60 mL min^{-1}. The energy consumption of the e-FO system (with a recirculation rate of 10 mL min^{-1}) for water extraction was significantly lower than other (lab-scale) emerging water recovery approaches such as microbial desalination cell (MDC, as low as 1.3 kWh m^{-3}) (Ping et al., 2015), bench-scale ED (7.0 kWh m^{-3}) (Walker et al., 2014), air gap membrane distillation (AGMD, 2.5–3.0 kWh m^{-3}) (Alkhudhiri et al., 2013), and the FO system with thermolytic ammonium bicarbonate (0.1 kWh m^{-3}) (Qin and He, 2014).

To better understand energy consumption interacted with reverse solute flux, the energy consumption of the power supply (E_s, kWh kg^{-1}, Supplementary Materials) and the whole system ($E_{s,total}$, kWh kg^{-1}, including both power supply and the recirculation pump) was normalized by the mass of the reduced reverse-fluxed solutes. As shown in Fig. 6C, the lowest E_s was 0.015 ± 0.002 kWh kg^{-1} with 1.5 V, while the highest was 2.280 ± 0.140 kWh kg^{-1} with 3 V. The $E_{s,total}$ of different recirculation rates with 1.5 V was presented in the inset of Fig. 6C. As expected, significant reduction of $E_{s,total}$ from 1.103 ± 0.059 kWh kg^{-1} to 0.044 ± 0.002 kWh kg^{-1} was obtained with decreasing the recirculation rate from 60 mL min^{-1} to 10 mL min^{-1}. Although the estimate of energy consumption in a bench-scale system cannot fully reflect that of a full-scale system for practical application (Xiang et al., 2017), it does provide implications that, to achieve mitigated RSF, electrolysis did not require significant energy input, and optimizing the operation of the e-FO system such as recirculation could save energy and thus offset the energy input by electrolysis. In addition, the benefits brought by RSF mitigation may compensate the cost increase induced by exerting voltage.

4. Conclusions

This study has demonstrated the feasibility of *in-situ* mitigation of RSF in a three-chamber electrolysis-assisted FO system. The effects of several operation parameters, e.g. applied voltage, membrane orientation, and initial draw solute concentration, were systematically examined and optimized towards maximizing RSF reduction. The results have important implications to further development of the electrolysis-assisted RSF mitigation within the e-FO system with the following conclusions:

- Applying a voltage of 1.5 V achieved a RSF of 6.78 ± 0.55 mmol m^{-2} h^{-1} and a specific RSF of 0.138 ± 0.011 g L^{-1} in the FO mode and with 1 M Na_2SO_4 as the draw, rendering ~57% reduction of solute leakage compared to the control without the applied voltage.
- The reduced RSF should be attributed to constrained ion migration induced by the coactions of electric dragging force (≥1.5 V) and high solute rejection of the FO membrane.
- Stable solution pH was achieved by continuous mixing of the anolyte and the catholyte towards prolonged lifespan of the FO membrane and electrodes in the e-FO system.
- Both membrane fouling and electrolysis-induced water loss (<0.001 mL L^{-1} recovered water) were negligible during the experiment. Reversible membrane fouling was well-controlled by *in-situ* osmotic backwashing with a flux recover rate of 98%.
- Reducing the intensity of the solution recirculation from 60 to 10 mL min^{-1} significantly reduced specific energy consumption of the e-FO system from 0.693 ± 0.127 to 0.022 ± 0.004 kWh m^{-3} extracted water or from 1.103 ± 0.059 to 0.044 ± 0.002 kWh kg^{-1} reduced reversed solute. Such an energy-efficient e-FO system could serve as a promising technology for sustainable water recovery and reuse.
- This e-FO system with *in-situ* RSF mitigation warrants further investigation of selected draw solutes and long-term implementation of real wastewater as a feed solution.

Acknowledgements

This research was financially supported by a grant from National Science Foundation (#1358145).

Appendix A. Supplementary data

Supplementary data related to this article can be found at http://dx.doi.org/10.1016/j.watres.2017.02.060.

References

Achilli, A., Cath, T.Y., Marchand, E.A., Childress, A.E., 2009. The forward osmosis membrane bioreactor: a low fouling alternative to MBR processes. Desalination 239 (1–3), 10–21.

Achilli, A., Cath, T.Y., Childress, A.E., 2010. Selection of inorganic-based draw solutions for forward osmosis applications. J. Membr. Sci. 364 (1), 233–241.

Alkhudhiri, A., Darwish, N., Hilal, N., 2013. Produced water treatment: application of air gap membrane distillation. Desalination 309, 46–51.

Bockris, J.O.M., Dandapani, B., Cocke, D., Ghoroghchian, J., 1985. On the splitting of water. Int. J. Hydrogen Energ 10 (3), 179–201.

Boo, C., Lee, S., Elimelech, M., Meng, Z., Hong, S., 2012. Colloidal fouling in forward osmosis: role of reverse salt diffusion. J. Membr. Sci. 390–391, 277–284.

Cath, T.Y., Childress, A.E., Elimelech, M., 2006. Forward osmosis: principles, applications, and recent developments. J. Membr. Sci. 281 (1), 70–87.

Cath, T.Y., Elimelech, M., McCutcheon, J.R., McGinnis, R.L., Achilli, A., Anastasio, D., Brady, A.R., Childress, A.E., Farr, I.V., Hancock, N.T., 2013. Standard methodology for evaluating membrane performance in osmotically driven membrane processes. Desalination 312, 31–38.

Chung, T.S., Li, X., Ong, R.C., Ge, Q., Wang, H., Han, G., 2012a. Emerging forward osmosis (FO) technologies and challenges ahead for clean water and clean energy applications. Curr. Opin. Chem. Eng. 1 (3), 246–257.

Chung, T.S., Zhang, S., Wang, K.Y., Su, J., Ling, M.M., 2012b. Forward osmosis processes: yesterday, today and tomorrow. Desalination 287, 78–81.

Hancock, N.T., Cath, T.Y., 2009. Solute coupled diffusion in osmotically driven membrane processes. Environ. Sci. Technol. 43 (17), 6769–6775.

Holloway, R.W., Achilli, A., Cath, T.Y., 2015. The osmotic membrane bioreactor: a critical review. Environ. Sci. Water Res. Technol. 1 (5), 581–605.

Le-Clech, P., Fane, A., Leslie, G., Childress, A., 2005. MBR focus: the operators' perspective. Filtr. Separat. 42 (5), 20–23.

Li, X., Lu, Y., He, Z., 2015. Removal of reverse-fluxed ammonium by anammox in a forward osmosis system using ammonium bicarbonate as a draw solute. J. Membr. Sci. 495, 424–430.

Liang, Y.Y., Fimbres Weihs, G.A., Wiley, D.E., 2016. CFD modelling of electro-osmotic permeate flux enhancement in spacer-filled membrane channels. J. Membr. Sci. 507, 107–118.

Ling, M.M., Wang, K.Y., Chung, T.-S., 2010. Highly water-soluble magnetic nanoparticles as novel draw solutes in forward osmosis for water reuse. Ind. Eng. Chem. Res. 49 (12), 5869–5876.

Ling, M.M., Chung, T.S., 2011a. Desalination process using super hydrophilic nanoparticles via forward osmosis integrated with ultrafiltration regeneration. Desalination 278 (1), 194–202.

Ling, M.M., Chung, T.S., 2011b. Novel dual-stage FO system for sustainable protein enrichment using nanoparticles as intermediate draw solutes. J. Membr. Sci. 372 (1), 201–209.

Liu, Z., Bai, H., Lee, J., Sun, D.D., 2011. A low-energy forward osmosis process to produce drinking water. Energy Environ. Sci. 4 (7), 2582–2585.

Lu, Y., He, Z., 2015. Mitigation of salinity buildup and recovery of wasted salts in a hybrid osmotic membrane bioreactor–electrodialysis system. Environ. Sci. Technol. 49 (17), 10529–10535.

Luo, W., Hai, F.I., Kang, J., Price, W.E., Nghiem, L.D., Elimelech, M., 2015. The role of forward osmosis and microfiltration in an integrated osmotic-microfiltration membrane bioreactor system. Chemosphere 136, 125–132.

McCutcheon, J.R., McGinnis, R.L., Elimelech, M., 2006. Desalination by ammonia–carbon dioxide forward osmosis: influence of draw and feed solution concentrations on process performance. J. Membr. Sci. 278 (1), 114–123.

Ng, H.Y., Tang, W., Wong, W.S., 2006. Performance of forward (direct) osmosis process: membrane structure and transport phenomenon. Environ. Sci. Technol. 40 (7), 2408–2413.

Nguyen, H.T., Nguyen, N.C., Chen, S.-S., Ngo, H.H., Guo, W., Li, C.W., 2015. A new class of draw solutions for minimizing reverse salt flux to improve forward osmosis desalination. Sci. Total Environ. 538, 129–136.

Nightingale Jr., E., 1959. Phenomenological theory of ion solvation. Effective radii of hydrated ions. J. Phys. Chem. 63 (9), 1381–1387.

Phillip, W.A., Yong, J.S., Elimelech, M., 2010. Reverse draw solute permeation in forward osmosis: modeling and experiments. Environ. Sci. Technol. 44 (13), 5170–5176.

Phuntsho, S., Shon, H.K., Hong, S., Lee, S., Vigneswaran, S., 2011. A novel low energy fertilizer driven forward osmosis desalination for direct fertigation: evaluating the performance of fertilizer draw solutions. J. Membr. Sci. 375 (1–2), 172–181.

Ping, Q., Huang, Z., Dosoretz, C., He, Z., 2015. Integrated experimental investigation and mathematical modeling of brackish water desalination and wastewater treatment in microbial desalination cells. Water Res. 77, 13–23.

Qin, M., He, Z., 2014. Self-supplied ammonium bicarbonate draw solute for achieving wastewater treatment and recovery in a microbial electrolysis cell-forward osmosis-coupled system. Environ. Sci. Technol. Lett. 1 (10), 437–441.

Qiu, C., Qi, S., Tang, C.Y., 2011. Synthesis of high flux forward osmosis membranes by chemically crosslinked layer-by-layer polyelectrolytes. J. Membr. Sci. 381 (1), 74–80.

Shaffer, D.L., Yip, N.Y., Gilron, J., Elimelech, M., 2012. Seawater desalination for agriculture by integrated forward and reverse osmosis: improved product water quality for potentially less energy. J. Membr. Sci. 415–416, 1–8.

Su, J., Zhang, S., Ling, M.M., Chung, T.S., 2012. Forward osmosis: an emerging technology for sustainable supply of clean water. Clean. Technol. Environ. 1–5.

Tuna, E., Kargi, F., Argun, H., 2009. Hydrogen gas production by electrohydrolysis of volatile fatty acid (VFA) containing dark fermentation effluent. Int. J. Hydrogen Energ 34 (1), 262–269.

Walker, W.S., Kim, Y., Lawler, D.F., 2014. Treatment of model inland brackish groundwater reverse osmosis concentrate with electrodialysis - Part II: sensitivity to voltage application and membranes. Desalination 345, 128–135.

Wang, H., Chung, T.S., Tong, Y.W., Jeyaseelan, K., Armugam, A., Chen, Z., Hong, M., Meier, W., 2012. Highly permeable and selective pore - spanning biomimetic membrane embedded with Aquaporin Z. Small 8 (8), 1185–1190.

Wang, J., Dlamini, D.S., Mishra, A.K., Pendergast, M.T.M., Wong, M.C., Mamba, B.B., Freger, V., Verliefde, A.R., Hoek, E.M., 2014a. A critical review of transport through osmotic membranes. J. Membr. Sci. 454, 516–537.

Wang, M., Wang, Z., Gong, X., Guo, Z., 2014b. The intensification technologies to water electrolysis for hydrogen production-A review. Renew. Sust. Energy Rev. 29, 573–588.

Xiang, X., Zou, S., He, Z., 2017. Energy consumption of water recovery from wastewater in a submerged forward osmosis system using commercial liquid fertilizer as a draw solute. Sep. Purif. Technol. 174, 432–438.

Xie, M., Zheng, M., Cooper, P., Price, W.E., Nghiem, L.D., Elimelech, M., 2015. Osmotic dilution for sustainable greenwall irrigation by liquid fertilizer: performance and implications. J. Membr. Sci. 494, 32–38.

Yuan, H., Abu-Reesh, I.M., He, Z., 2016. Mathematical modeling assisted investigation of forward osmosis as pretreatment for microbial desalination cells to achieve continuous water desalination and wastewater treatment. J. Membr. Sci. 502, 116–123.

Zou, S., He, Z., 2016. Enhancing wastewater reuse by forward osmosis with self-diluted commercial fertilizers as draw solutes. Water Res. 99, 235–243.

Zou, S., Yuan, H., Childress, A., He, Z., 2016. Energy consumption by recirculation: a missing parameter when evaluating forward osmosis. Environ. Sci. Technol. 50 (13), 6827–6829.